Irganox 3114 was identified in all three extracts, based on the quasimolecular ions observed in the positive ion spectra and fragment ions in the negative ion spectra. Naugard 524 is believed to be present based on a fragment in the negative ion spectrum, which was determined by exact mass measurement to be a reasonable oxidation/hydrolysis product of Naugard 524, and the presence in the positive ion spectrum of quasimolecular ions corresponding to the phosphate oxidation product of Naugard 524. DSTDP is tentatively identified in the tarp extract. A database containing molecular weights of likely additives would be very useful, since most additives were found to give strong quasimolecular ions under defocused laser desorption conditions. While reference spectra are not needed, they can provide strong confirmation of an additive identity through fragment ion information.

LITERATURE CITED

(1) Sevini, F.; Marcato, B. *J. Chromatogr.* **1983**, *260*, 507-512.
(2) Haney, M. A.; Dark, W. A. *J. Chromatogr. Sci.* **1980**, *18*, 655-659.
(3) Munteanu, D.; Isfan, A.; Isfan, C.; Tincul, I. *Chromatographia* **1987**, *23*, 7-14.
(4) Perlstein, P. *Anal. Chim. Acta* **1983**, 21-27.
(5) Schabron, J. F.; Fenska, L. E. *Anal. Chem.* **1980**, *52*, 1411-1415.
(6) Raynor, M. W.; Barle, K. D.; Davies, I. L.; Williams, A.; Clifford, A. A.; Chalmers, J. M.; Cook, B. W. *Anal. Chem.* **1988**, *60*, 427-433.
(7) Vargo, J. D.; Olson, K. L. *Anal. Chem.* **1985**, *57*, 672-675.
(8) Lattimer, R. P.; Harris, R. E.; Rhee, C. K. *Anal. Chem.* **1986**, *58*, 3188-3195.
(9) Lattimer, R. P.; Harris, R. E. *Mass Spectrom. Rev.* **1985**, *4*, 369-390.
(10) Hsu, A. T.; Marshall, A. G. *Anal. Chem.* **1988**, *60*, 932-937.
(11) Blease, T. G.; Scrivens, J. H.; Monaghan, J. J.; Weil, D. Presented at the 36th ASMS Conference on Mass Spectrometry and Allied Topics, San Francisco, CA, June 5-10th, 1988; paper MPB 73.
(12) Wilkins, C. L.; Laude, D.; Pentoney, S.; Griffiths, P. R.; The University of California, Riverside, private communication, 1987.
(13) Cody, R. B. *Anal. Chem.* **1988**, *60*, 917-923.
(14) Wise, M. B. *Anal. Chem.* **1987**, *59*, 2289-2293.
(15) Kresser, T. O. J. *Polyolefin Plastics*; Van Nostrand Reinhold: New York, 1969; pp 56-63.
(16) Wilk, Z. A.; Viswanadham, S. K.; Sharkey, A. G.; Hercules, D. M. *Anal. Chem.* **1988**, *60*, 2338-2346.
(17) Chiarelli, M. P.; Gross, M. L. I. *J. Mass Spectrom. Ion Processes* **1987**, *78*, 37-52.
(18) Cotter, R. J.; Tabet, J.-C. *Am. Lab.* **1984**, *4*, 86-99.
(19) Hercules, D. M. *Microchem. J.* **1988**, *38*, 3-23.
(20) Asamoto, B. *Spectroscopy* **1988**, *6*, 38-46.
(21) *Stabilization of Polymers and Stabilizer Processes*; Gould, R. F., Ed.; Advances in Chemistry 85; American Chemical Society: Washington, DC, 1968; p 209.

RECEIVED for review October 3, 1989. Accepted October 18, 1989.

Precise Relative Ion Abundances from Fourier Transform Ion Cyclotron Resonance Magnitude-Mode Mass Spectra

Zhenmin Liang and Alan G. Marshall*,[1]

Department of Chemistry, The Ohio State University, 120 West 18th Avenue, Columbus, Ohio 43210

The area under a correctly phased absorption-mode spectral peak is a direct measure of the number of oscillators (ions, spins, molecules) in Fourier transform spectrometry (ion cyclotron resonance, magnetic resonance, interferometry absorbance). However, phase correction can prove difficult when (as in broad-band Fourier transform ion cyclotron resonance (FT/ICR)) detection is considerably time-delayed after excitation. In the absence of noise, Huang, Rempel, and Gross showed that a "complex area" method yields the correct absorption-mode peak area, for an unphased noiseless spectrum. In this paper, we show that the number of oscillators may also be obtained from a least-squares fit to a magnitude-mode (i.e., phase-independent) spectrum. In the presence of noise and in the absence of peak overlap, the magnitude-mode method offers precision superior to that based on magnitude-mode peak height, "complex area", or even direct digital integration of a correctly phased absorption-mode peak, as demonstrated by both theoretical derivation and experimental FT/ICR results. The present method thus appears to offer the best available determination of the relative abundances of ions of different mass-to-charge ratio in FT/ICR mass spectrometry.

INTRODUCTION

One of the most fundamental uses of Fourier transform (FT) spectroscopy is to determine the relative numbers of different species from relative spectral peak "intensities". Most FT spectroscopists use absorption-mode spectral peak *height* as a measure of the number of oscillators at that frequency. [In FT/interferometry, the detector measures light *energy*, not its *electric field*. However, because of the (nonlinear) square-law detection process, an FT of an interferogram nevertheless yields a complex intensity spectrum which when correctly phased yields absorption-mode and dispersion-mode (not "power") spectra (*1*).] Unfortunately, relative oscillator abundances are related to relative peak heights only if all spectral peaks have identical *widths*. In a frequency-domain spectrum obtained by discrete Fourier transformation (FFT) of the time-domain response immediately following a delta-function excitation, the absorption-mode spectral peak relative *areas* are directly proportional to the time-domain relative initial *amplitudes* of the time-domain sinusoidal signals, which in turn are proportional to the numbers of oscillators at those frequencies (*1*). In other words, one should use FT absorption-mode spectral peak *areas* rather than peak *heights* as the proper measure of relative abundances of spectral components.

However, it is not always possible to phase-correct a complex FT spectrum to obtain its pure absorption-mode component. For example, when the time-domain detection must be delayed by more than half of one sampling period after excitation (e.g., to avoid feed-through of the excitation signal into the detector channel), then the failure of the FFT algorithm to accommodate a phase variation of more than 2π radians throughout the spectral range results in FFT spectral phase discontinuities ["phase-wrap" (*1*, *2*)] which produce unavoidable auxiliary "wiggles" in each spectral peak, even for a perfectly phased spectrum. The phase-wrap "wiggles"

* To whom correspondence should be addressed.
[1] Also a member of the Department of Biochemistry.

0003-2700/90/0362-0070$02.50/0

have the same form as those from "Gibb's oscillations" resulting from truncation of a time-domain exponentially damped sinusoid before FFT, but the "phase-wrap" effect is unique to the *discrete* FT, whereas "Gibb's oscillations" are present even in *analog* FT of a continuous time-domain signal (*1*, *2*). Other instrumental anomalies can produce nonlinear phase shift as a function of frequency. In such cases, the phase-independent magnitude-mode spectral display is usually preferred.

Unfortunately, even in the absence of peak overlap (which is more pronounced for magnitude-mode than for absorption-mode display), magnitude-mode peak height is not a good measure of relative oscillator abundances since peak widths commonly vary significantly. Moreover, magnitude-mode peak area is unsuitable, because (a) if the domain of integration is extended to infinity, magnitude-mode peak area diverges to infinity for a simple Lorentz line shape (*3*), and (b) if the domain of integration is truncated to a finite frequency range, then the relative peak areas will be accurate only if all of the peak widths are the same. Thus, directly integrated magnitude-mode peak relative areas offer a poor measure of relative oscillator abundances.

Although three-point interpolation of a noiseless magnitude-mode FT spectrum can yield the frequency of the peak maximum exactly (*4*, *5*), the peak height and area are not so easily estimated, and both estimates are corrupted by noise (*6*, *7*). In addition, the apparent frequency and height of a magnitude-mode peak can be shifted significantly by the presence of nearby peaks, to a greater extent than for absorption-mode spectra (because of the dispersion-mode contribution to the magnitude-mode spectrum) (*8*, *9*).

Another set of difficulties with magnitude-mode display relates to the nature of magnitude-mode noise. First, since magnitude-mode noise is everywhere positive-valued, noise can quickly overwhelm the signal if the peak area computation is extended very far away from the center of the magnitude-mode spectral peak. Furthermore, magnitude-mode noise (in the absence of signal) follows a Rayleigh rather than Gaussian distribution (*10*). Moreover, magnitude-mode noise contributes only positive errors in spectral segments containing no signal (i.e., "base line") but contributes both positive and negative errors in spectral segments where signals (i.e., "peaks") are present. In work to be reported separately, statistical criteria used to analyze the noise in signal-containing segments of a magnitude-mode spectrum show that such noise is *not* well-described by a Rayleigh distribution (*11*).

In an effort to circumvent the problems posed by magnitude-mode spectral analysis, Huang, Rempel, and Gross proposed a "complex area" method, to calculate the absorption peak area from unphased (noiseless) spectra (*12*). Alternatively, comparison of FT spectra of partial segments of a discrete time-domain signal (*13*, *14*) also provides a means for correcting for spectral peak height variations due to differences in peak width. Noest and Kort (*15*) have suggested a time-domain apodization function designed to produce spectral peaks with broad and flat peak maxima, to reduce errors due to discrete sampling. The value of linear prediction (*16*) and/or maximum-entropy methods for analysis of FT/ICR mass spectra is discussed elsewhere (*17*). Apparent relative abundances of ions in FT/ICR can of course also be affected by various experimental factors, including z-axis ejection (*18–20*), collisional relaxation of ions to the center of the ion trap (*21*), incomplete ejection of unwanted ions (*21*), and phase and amplitude errors (*22*).

Under quite general conditions (white noise whose root-mean-square magnitude is independent of signal magnitude), we have shown that the precision of a determination of spectral peak height, peak width, or peak center frequency by least-squares fit to an absorption-mode or magnitude-mode spectrum is proportional to the frequency-domain signal-to-noise ratio (SNR) and to the square root of the number of data points (K) per line width (*23*)

$$P(a_i) = c(a_i)\ \mathrm{SNR}\ K^{1/2} \tag{1}$$

in which a_i is the spectral peak height, peak width, or peak center frequency and $c(a_i)$ is a line shape-dependent constant factor.

We begin this paper by extending that treatment to show that the precision of the *number of oscillators* determined by least-squares fit to a magnitude-mode spectrum (or by digital integration of the absorption spectrum, or by the above-cited complex area method) is also proportional to SNR and $K^{1/2}$, with an appropriate value of $c(a_i)$ in eq 1. By comparing the proportionality constants, $c(a_i)$, we are then able to evaluate the relative precision of each of the above methods for peak area determination. Finally, we compare simulated and experimental FT/ICR spectra to demonstrate the validity of our analysis. [We shall report separately on the closely related problem of precision in determination of the same parameters (peak height, width, frequency, and number of oscillators) from a discrete *time-domain* signal, including the effect of time-domain zero-filling (*11*).]

THEORY

Magnitude-Mode Noise. Magnitude-mode spectral noise differs fundamentally from noise in absorption-mode or dispersion-mode spectra. Although noise in signal-free segments of a magnitude-mode spectrum follows a Rayleigh distribution (*10*), magnitude-mode noise at or near peaks more than 2 standard deviations above the base line is more nearly Gaussian-distributed (*11*). In a separate paper, we shall discuss magnitude-mode noise in detail, and show that a least-squares fit to a magnitude-mode spectral peak may be performed with high precision under the assumption that the noise in the vicinity of the peak is Gaussian-distributed about a zero mean value (*11*).

Precision of Peak Area Measurements. *1. Least-Squares Fit to a Frequency-Domain Spectrum.* The number of oscillators can be determined by numerical integration (of either a phased absorption-mode peak or "complex area" (*12*)) or from a least-squares fits to either the absorption-mode peak or magnitude-mode spectrum. In any case, we begin from the absorption-mode, Abs(ν), and magnitude-mode, Mag(ν), Lorentzian frequency-domain spectra corresponding to the Fourier transform of an unapodized time-domain exponentially damped sinusoid, $f(t)$

$$f(t) = N_0 \exp(-t/\tau) \sin(2\pi\nu_0 t) \tag{2}$$

$$\mathrm{Abs}(\nu) = \frac{N_0\tau}{2[1 + (2\pi\tau)^2(\nu - \nu_0)^2]} = \frac{N_0\tau}{2[1 + u^2]} \tag{3}$$

$$\mathrm{Mag}(\nu) = \frac{N_0\tau}{2(1 + (2\pi\tau)^2(\nu - \nu_0)^2)^{1/2}} = \frac{N_0\tau}{2(1 + u^2)^{1/2}} \tag{4}$$

in which $u = 2\pi\tau(\nu - \nu_0)$; N_0 is the time-domain signal initial magnitude, which is proportional to the number of ions having that ICR frequency; $N_0/4$ is the area under the Lorentzian absorption-mode spectra peak; $N_0\tau/2$ is the Lorentzian absorption-mode peak height; $\tau = 1/\pi\,\Delta\nu_{1/2}$, time-domain ICR signal damping constant (see eq 2); $\Delta\nu_{1/2}$ is the absorption-mode full peak width at half maximum peak height; and ν_0

is the ICR frequency, the frequency at the absorption-mode or magnitude-mode peak maximum.

The object of this paper is to be able to predict, from a *single* FT magnitude-mode spectrum, the *precision* of the determined number of oscillators (i.e., a measure of the range of values that would have been obtained from a *large number* of such measurements). Precision, $P(N_0)$, in determination of number of oscillators may be defined as the reciprocal of the relative standard error

$$P(N_0) = N_0/\sigma(N_0) \tag{5}$$

in which $\sigma(N_0)$ is the standard deviation that would be obtained from many independent determinations of N_0. If the absorption-mode spectral noise is "white" (i.e., independent of frequency) and independent of signal (i.e., "detector-limited") and if the time- and frequency-scales are perfectly precise (i.e., noise is present only in the ordinate, not in the abscissa), then the precision, $P(a_i)$, in a determination of spectral parameter, a_i, from a least-squares fit of the spectrum to a given line shape can be shown to be (*23*)

$$P(a_i) = c(a_i)\,(\mathrm{SNR})\,K^{1/2} \tag{1}$$

in which $c(a_i)$ is a line-shape-dependent constant, K is the number of data points per (full) line width at half-maximum peak height, and SNR is the spectral signal-to-noise ratio, which for Lorentzian line shape takes the form

$$\mathrm{SNR} = N_0\tau/2\sigma \tag{6}$$

in which σ is the standard deviation of the absorption-mode spectral base-line noise.

Reference 23 presents a general method for deriving $c(a_i)$ for $a_i = \nu_0$, peak height, or peak width, for Lorentzian or Gaussian absorption-mode and magnitude-mode spectra. In this work, we have applied that method to three-parameter (N_0, ν_0, and τ) least-squares fits to Lorentzian absorption-mode and magnitude-mode line shapes to yield

$$c(N_0) = \left(\frac{\pi}{8}\right)^{1/2} \tag{7a}$$

for Lorentzian absorption-mode line shape and

$$c(N_0) = \left(\frac{\pi}{6(3)^{1/2}}\right)^{1/2} \tag{7b}$$

for Lorentzian magnitude-mode line shape.

In the special case that τ is known accurately (e.g., from measurement of the width of a peak of high SNR in a spectrum for which all of the peaks have the same line width), then it can be shown that the resulting precision in a two-parameter (N_0 and ν_0) least-squares determination of N_0 increases by a factor of $2^{1/2}$ for an absorption-mode and $3^{1/2}$ for a magnitude-mode Lorentzian, compared to a three-parameter fit (N_0, ν_0, and τ).

Finally, it is worth noting that because the magnitude-mode Lorentzian line width (at half-maximum peak height) is broader than the absorption-mode Lorentzian line width by a factor of $3^{1/2}$, the number of data points per line width increases by $3^{1/2}$ and the precision as defined above therefore increases by $K^{1/2} = 3^{1/4}$ for magnitude-mode. Therefore, if we choose to express K as number of points per frequency increment rather than number of points per line width (to facilitate comparison of absorption-mode and magnitude-mode precision), then $C(N_0)$ for magnitude-mode fits should be increased by the factor $3^{1/4}$ (see below).

2. Digital Integration of a Phase-Corrected Absorption-Mode Spectral Peak. From the standpoint of precision, a numerical integration (independent of algorithm) of an absorption-mode spectrum is equivalent to summing up all of the absorption values within the integral limit and multiplying by the discrete frequency interval, $\Delta\nu$, between successive frequency-domain absorption-mode data. Therefore, the deviation, δ, in such an integral is defined by

$$\delta = \sum_{i=0}^{n}[\mathrm{Abs}(\nu_i) + N(\nu_i)]\,\Delta\nu - \sum_{i=0}^{n}\mathrm{Abs}(\nu_i)\,\Delta\nu = \sum_{i=0}^{n}N(\nu_i)\,\Delta\nu \tag{8}$$

in which $\mathrm{Abs}(\nu_i)$ and $N(\nu_i)$ are the (absorption-mode) signal and noise values at (discrete) frequency ν_i, and noise is assumed independent of signal. δ is normally distributed with zero mean and standard deviation

$$\sigma(\mathrm{area}) = n^{1/2}\sigma\,\Delta\nu \tag{9}$$

in which n is the number of absorption-mode data points in the integration domain (*24*). Next, since N_0 and absorption-mode peak area differ by a constant (see eq 4 ff)

$$P(N_0) = \frac{N_0}{\sigma(N_0)} = \frac{\text{absorption area}}{\sigma(\text{absorption area})} \tag{10}$$

Then, since the absorption-mode peak area is $N_0/4$, we can use eq 9 to obtain

$$P(N_0) = \frac{\text{absorption area}}{\sigma(\text{absorption area})} = \frac{N_0}{4n^{1/2}\sigma\,\Delta\nu} \tag{11}$$

Next, solve eq 6 for N_0 and substitute for N_0 in eq 11; then substitute for $\tau = 1/(\pi\,\Delta\nu_{1/2})$ to obtain the following expression for the precision in determination of N_0 from a measurement of absorption-mode Lorentzian peak area

$$P(N_0) = \frac{\pi}{2h^{1/2}}(\mathrm{SNR})K^{1/2} \tag{12a}$$

in which

$$h = n/K \tag{12b}$$

is the domain of integration (in multiples of $\Delta\nu_{1/2}$) and we have used the identity

$$K(\text{points/line width}) = \frac{\Delta\nu_{1/2}(\text{Hz/line width})}{\Delta\nu(\text{Hz/point})} \tag{12c}$$

For eq 12a to be valid, the domain of numerical integration should be chosen so as to include, say, >95% of the true absorption-mode peak area.

3. "Complex Area". The "complex" area method consists of adding the areas (each treated as mathematically real quantities) of the real, $R(\nu_i)$, and imaginary, $I(\nu_i)$, spectra obtained by discrete FT of a time-domain discrete signal (*12*). In this case, the deviation in the resultant area is given by

$$\delta = \Delta\nu(([\sum_{i=1}^{n}R(\nu_i) + N_\mathrm{R}(\nu_i)]^2 + [\sum_{i=1}^{n}I(\nu_i) + N_\mathrm{I}(\nu_i)]^2)^{1/2} - ([\sum_{i=1}^{n}R(\nu_i)]^2 + [\sum_{i=1}^{n}I(\nu_i)]^2)^{1/2})$$

$$\approx \Delta\nu([\sum_{i=1}^{n}R(\nu_i)]^2 + [\sum_{i=1}^{n}I(\nu_i)^2 + 2N'_\mathrm{R}(\nu_i)[\sum_{i=1}^{n}R(\nu_i)] + 2N'_\mathrm{I}(\nu_i)[\sum_{i=1}^{n}I(\nu_i)])^{1/2} - ([\sum_{i=1}^{n}R(\nu_i)]^2 + [\sum_{i=1}^{n}I(\nu_i)]^2)^{1/2} \tag{13}$$

in which

$$N'_\mathrm{R}(\nu_i) = \sum_{i=1}^{n}N_\mathrm{R}(\nu_i) \tag{14a}$$

and

$$N'_I(\nu_i) = \sum_{i=1}^{n} N_I(\nu_i) \quad (14b)$$

represent randomly distributed Gaussian noise (with standard deviation $\sigma n^{1/2}$) in the real and imaginary spectral components of the complex FFT of $f(t)$ (*24*), and we have used the approximation

$$2N'_R(\nu_i)\sum_{i=1}^{n} R(\nu_i) + 2N'_I(\nu_i)\sum_{i=1}^{n} R(\nu_i) \gg N'_R(\nu_i)^2 + N'_I(\nu_i)^2 \quad (15)$$

If equation 13 is next expanded in a Taylor series and only the first two terms are kept—neglect of the remaining terms produces negligible error in practical circumstances—then eq 13 may be simplified to give

$$\delta = \frac{N_R(\nu_i)\sum_{i=1}^{n} R(\nu_i) + N_I(\nu_i)\sum_{i=1}^{n} I(\nu_i)}{([\sum_{i=1}^{n} R(\nu_i)]^2 + [\sum_{i=1}^{n} I(\nu_i)]^2)^{1/2}} \quad (16)$$

In other words, δ may be described by a normal distribution with zero mean and standard deviation, $\sigma n^{1/2}$, which is the same as for direct numerical integration of a perfectly phased absorption-mode spectrum (*19*). Thus, for numerical integration of either phased absorption-mode or "complex area", the precision in determination of absorption-mode peak are is given by

$$P(N_0) = \frac{\pi}{2h^{1/2}}(\mathrm{SNR})K^{1/2} \quad (12a)$$

EXPERIMENTAL SECTION

Simulated Data. Data simulation was conducted with a 20 bit/word Nicolet 1280 computer. Gaussian noise was created by converting uniform random numbers into a Gaussian distributed random number file (*25*). The histogram of the Gaussian random numbers closely resembled that for experimentally acquired Gaussian noise, and the FFT spectrum of the random number sequence showed no peaks [demonstrating that the noise was "white" (i.e., independent of frequency)]. Random noise was added to each time-domain simulated signal, and least-squares fit to a magnitude-mode Lorentzian line shape was performed on the FFT spectrum of the time-domain simulated signal-plus-noise.

Experimental Data. FT/ICR experimental time-domain signals of I_2^+ were acquired with a Nicolet FTMS-2000 mass spectrometer operating in heterodyne mode at 3 T. Iodine crystals were introduced with a solid probe which had been cooled to ~10 °C, and I_2^+ ions were formed by electron ionization (70 eV). The number of points per line width in the FFT spectrum was adjusted by varying the sampling frequency (32 kHz < Nyquist bandwidth < 100 kHz) while keeping the number of time-domain data points constant (4K or 8K). Alternatively, the time-domain damping constant was varied [by addition of argon gas to a neutral pressure between 10^{-6} Torr ($\tau \approx 20$ ms) and 10^{-7} Torr ($\tau \approx 200$ ms)] at fixed sampling rate and number of time-domain data points, to cover the same abscissa range in Figures 3 and 4 (see Results and Discussion). Signal-to-noise ratio was additionally varied by varying the electron emission current. The number of points per line width in the FFT spectrum was adjusted by varying the sampling frequency at constant time-domain acquisition period. The standard deviation for ion relative abundance (determined from FT/ICR mass spectral peak area) was computed from 15 spectra acquired independently under identical conditions. The (single-peak) spectra were phase corrected before performing absorption-mode least-squares fit or numerical integration.

Least-squares fits to both magnitude-mode and absorption-mode spectra were performed with a grid search algorithm (*25*). An initial estimate for the fit parameters (peak area, peak center frequency, and peak width) was obtained by visual approximation from the magnitude-mode spectrum. A representative experimental FT/ICR magnitude-mode discrete spectrum and best-fit Lorentzian are shown in Figure 5 (see Results and Discussion).

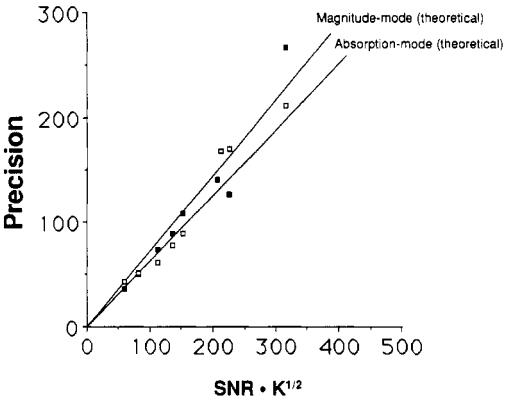

Figure 1. Precision in determination of number of oscillators, N_0, as a function of the ratio, SNR, of frequency-domain peak height to root mean square spectral base-line noise, and number of data points, K, per full peak width at half-maximum absorption-mode peak height: □, direct least-squares fit to absorption-mode spectrum; ■, direct least-squares fit to magnitude-mode spectrum. Straight lines are theoretical predictions based on a *single* (simulated) data set. Plotted data represent averages over 30 trials of the same simulated spectrum with different random noise of the same root mean square deviation.

Numerical integration of the phase-corrected absorption-mode spectrum was performed by use of Simpson's rule (*25*). Complex area was obtained as described by Gross (*12*).

RESULTS AND DISCUSSION

Computer-Simulated Spectra. The predicted precision in determination of number of oscillators was computed from eq 1 and 7 (based on fits to absorption-mode or magnitude-mode Lorentzian peak shape) or eq 12a (for direct integration of phased absorption-mode or "complex area") for simulated spectra with various frequency-domain signal-to-noise ratios (SNR) and K values. Those predictions were tested by determining the standard deviation for various spectral parameters (absorption-mode peak area, ν_0, and τ) from 30 simulated spectra of the same spectral peak height, ν_0, and τ, with different added random noise of the same root-mean-square deviation.

Figure 1 compares the precision, $P(N_0)$, in determination of the number of oscillators predicted from a single spectrum to that actually computed from the standard deviation of 30 such measurements of the FFT spectra of simulated time-domain damped exponential sinusoidal signals to which random time-domain noise has been added. In the figure, $P(N_0)$ based on three-parameter (peak area, ν_0, and τ) fits to Lorentzian absorption-mode and magnitude-mode spectra is plotted as a function of the product of frequency-domain peak height-to-noise ratio (SNR) and $K^{1/2}$. For absorption mode, K is the number of points per full absorption-mode peak width at half-maximum peak height. For magnitude mode, K is redefined as $3^{1/4}$ times the number of points per absorption-mode peak width, in order that the absorption-mode and magnitude-mode plots may be compared on the basis of points per hertz rather than points per line width. Figure 2 shows the corresponding plots of precision vs $(\mathrm{SNR})(K/h)^{1/2}$ for numerical integration of a correctly phased Lorentzian absorption-mode spectrum or a "complex area" integration; in each case, the domain of integration is extended to include 95% of the peak area.

According to the theory, N_0 determined from least-squares fit to a magnitude mode spectrum is ~15% more precise than N_0 determined from least-squares fit to the corresponding absorption-mode spectrum, because (a) the number of points per peak width increases by $3^{1/2}$ in proceeding from absorption-mode to magnitude-mode Lorentzian line shape (so that K increases by $3^{1/2}$ and the precision increases by $K^{1/2}$, for a net increase in precision of ~30%) and (b) the magni-

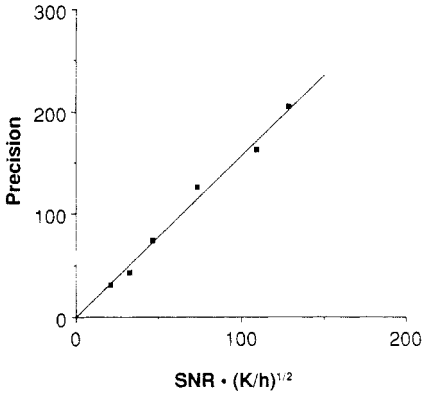

Figure 2. As in Figure 1, except that the number of data points per line width has been divided by the number of line widths, h, over which peak area is measured: □, N_0 determined from the sum of the areas of the real and imaginary components of the complex FFT spectrum (*12*); ■, N_0 determined from (phased) absorption-mode spectral peak area by direct numerical integration. Note: the open and solid squares overlap so closely that they cannot be resolved in this display.

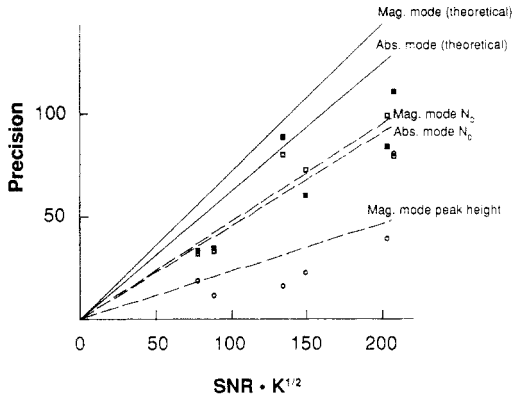

Figure 3. Same as Figure 1, but for experimental FT/ICR mass spectral data: □, direct least-squares fit to absorption-mode spectrum; ■, direct least-squares fit to magnitude-mode spectrum; O, N_0 determined from peak height of least-squares fit to magnitude-mode spectrum; ——, theoretically predicted behavior for the stated experimental SNR and K values; – – –, straight line passing through the origin which best fits the plotted points.

tude-mode peak shape is different from absorption mode, leading to a different value of $c(a)$. (The magnitude-mode fit extends to frequencies at which the spectral signal has dropped to twice the root-mean-square base-line noise.)

To compare the precision of the least-squares fits to the direct numerical integration methods, we must fix the domain of integration, h. For example, if the direct integration is to include 95% or more of the absorption-mode peak area, h must be greater than 12.7 absorption-mode Lorentzian line widths. Under those conditions, *the magnitude-mode least-squares fit is 60% more precise than numerical integration of either the phase corrected spectrum or the "complex area" method.* The simulated spectral data analyzed in Figures 1 and 2 thus confirm the theoretical predictions of eq 1 and 7 (for least-squares fits) and eq 12a (for direct integration).

One might argue that when only *relative* abundances are required, the integration width need not extend to include 95% of the absorption-mode peak area, thereby increasing the precision of the direct integratioin method. However, partial integration presents two practical problems. First, unless the peak widths (i.e., τ values) of all of the peaks are identical, systematic errors in relative abundances will be introduced. Second, the increase in precision, area/σ(area), by reduction in integration domain, h, will be small, because a decrease in h reduces the computed area as well as the

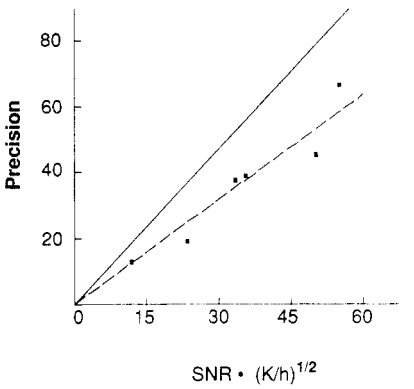

Figure 4. Same as Figure 2, but for experimental FT/ICR data. Again, the open and solid squares overlap in this display; ——, theoretically predicted behavior for the stated experimental SNR and K values; – – –, straight line passing through the origin which best fits the plotted points.

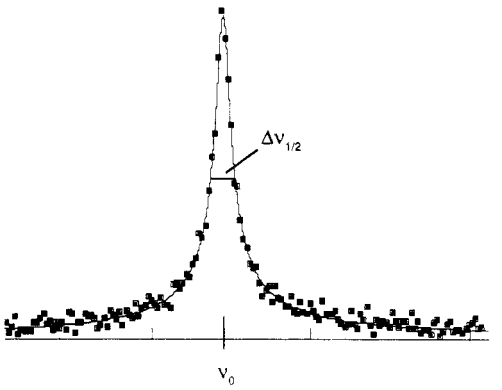

Figure 5. Representative discrete magnitude-mode FT/ICR mass spectrum, with best-fit magnitude-mode Lorentzian smooth curve drawn through the points.

imprecision in area measurement: $\sigma(\text{area}) \propto h^{1/2}$.

Experimental FT-ICR Spectra Figures 3 and 4 present experimental FT/ICR mass spectral data for I_2^+ ions, plotted as for the simulated data of Figures 1 and 2. Figure 5 shows a typical experimental magnitude-mode FT/ICR discrete mass spectrum along with a best-fit to magnitude-mode Lorentz line shape. The theoretical lines in Figures 3 and 4 represent predicted precision based on SNR and K for a *single* spectrum, and the data points represent the actual precision in N_0 determined from a *series* of 15 independent measurements. Although the slopes of plots of peak area precision vs SNR$K^{1/2}$ from experimental data are 20–30% lower than those predicted for the theoretical ones, the data still give straight-line plots with correlation coefficients of ≥0.9. The differences between experiment and theory are probably due mainly to variation in number of ions from one experiment to the next, due to variation in electron beam current. Nevertheless, Figures 3 and 4 show that the precision in N_0 determined from least-squares fit to a magnitude spectrum is slightly better than that for N_0 determined from a least-squares fit to the corresponding absorption-mode spectrum and is ~60% better than that for N_0 determined by "complex area" or direct numerical integration of a phased absorption-mode spectrum (for integration domain extended to include 95% of the peak area).

Finally, Figure 3 (open circles) illustrates the disadvantage of the use of peak *height* as a measure of relative abundances. Although theory predicts (compare the present results with those in ref 23) that the precision in peak *height* should be as good as that for peak *area* (provided that all spectral peak *widths* are equal), Figure 3 shows that for experimental FT/ICR data, relative abundance computed from least-squares fit to spectral data points whose magnitude exceeded

$\sim 2\sigma$ is twice as precise as relative abundance obtained simply from peak *height* of the same least-squares-fitted magnitude-mode spectrum.

Althought the present computations are restricted to *unapodized* magnitude-mode Lorentzian line shapes, the same qualitative conclusions should apply to other line shapes, with revised values of $c(a_i)$ in eq 1 (see ref 23 for examples).

CONCLUSION

In this paper, we have developed expressions for the precision of number of oscillators, N_0, obtained by various treatments of FFT absorption-mode and magnitude-mode Lorentzian spectra. We find that both theoretical and experimental FT/ICR relative abundance precision based on least-squares fit to the magnitude-mode spectrum is slightly more precise than that obtained from least-squares fit to the corresponding (if available) phased absorption-mode spectrum. Although both of the above methods are distinctly superior in precision to determination of N_0 by direct numerical integration of the complex or phased imaginary (i.e., pure absorption-mode) FFT spectrum, the magnitude-mode approach has the (major) advantage that it is not necessary to phase-correct the spectrum in order to determine relative abundances. (It is worth noting that the "complex area" computation requires twice as much memory as a magnitude-mode least-squares fit.) Experimental FT/ICR precision in N_0 is somewhat ($\sim 20\%$) lower, for all algorithms, than that predicted theoretically. Finally, peak *area* is in general superior to peak *height* as a measure of relative abundances.

LITERATURE CITED

(1) Marshall, A. G.; Verdun, F. R. *Fourier Transforms in Optical, NMR, and Mass Spectroscopy*; Elsevier: Amsterdam, 1989.
(2) Craig, E.; Marshall, A. G. *J. Magn. Reson.* **1988**, *76*, 458–475.
(3) Shaw, D. *Fourier Transform N.M.R. Spectroscopy*, 2nd ed.; Elsevier: Amsterdam, 1984; p 171.
(4) Giancaspro, C.; Comisarow, M. B. *Appl. Spectrosc.* **1983**, *37*, 153–166.
(5) Keefe, C. D.; Comisarow, M. B. *Appl. Spectrosc.* **1989**, *43*, 605–607.
(6) Chan, S. O.; Comisarow, M. B. *J. Magn. Reson.* **1983**, *54*, 201–215.
(7) Verdun, F. R.; Giancaspro, C.; Marshall, A. G. *Appl. Spectrosc.* **1988**, *42*, 715–721.
(8) Lee, J. P.; Chow, K. H.; Comisarow, M. B. *Anal. Chem.* **1988**, *60*, 2212–2218.
(9) Chow, K. H.; Comisarow, M. B. *Int. J. Mass Spectrom. Ion Processes* **1989**, *89*, 187–203.
(10) Hanna, D. A. 33rd American Society of Mass Spectrometry Annual Conference on Mass Spectrometry and Allied Topics, San Diego, CA, May, 1985; Collected Abstracts, pp 435–436.
(11) Liang, Z.; Marshall, A. G. 37th American Society of Mass Spectrometry Annual Conference on Mass Spectrometry and Allied Topics, Miami Beach, FL, May 1989; Collected Abstracts, pp 1234–1235. Dunbar, R. C., private communication.
(12) Huang, S. K.; Rempel, D. L.; Gross, M. L. American Society of Mass Spectrometry 32nd Annual Conference on Mass Spectrometry and Allied Topics, San Antonio, TX, May 1984; Collected Abstracts, pp 596–597.
(13) de Koning, L. J.; Kort, C. W. F.; Pinske, F. A.; Nibbering, N. M. M. *Int. J. Mass Spectrom. Ion Processes*, in press.
(14) Mitchell, D. W.; DeLong, S. E. *Int. J. Mass Spectrom. Ion Processes*, in press.
(15) Noest, A. J.; Kort, C. W. F. *Comput. Chem.* **1982**, *6*, 115–119.
(16) Rahbee, A. *Int. J. Mass Spectrom. Ion Processes* **1986**, *72*, 1–14.
(17) Meier, J. E.; Marshall, A. G. *Anal. Chem.*, in press.
(18) Rempel, D. L.; Huang, S. K.; Gross, M. L. *Int. J. Mass Spectrom. Ion Processes* **1986**, *70*, 163–184.
(19) Van der Hart, W. J.; Van de Guchte, W. J. *Int. J. Mass Spectrom. Ion Processes* **1988**, *82*, 17–31.
(20) Wang, M.; Marshall, A. G. 37th Amer. Soc. Mass Spectrom. Annual Conf. on Mass Spectrom. & Allied Topics, Miami Beach, FL, May, 1989; Collected Abstracts, pp 1226–1227; Hanson, C. D.; Castro, M. E.; Russell, D. H. *Ibid.* pp 1274–1275.
(21) Moini, M.; Eyler, J. R. *Int. J. Mass Spectrom. Ion Processes* **1989**, *87*, 29–40.
(22) Poretti, M.; Rapin, J.; Gäumann, T. *Int. J. Mass Spectrom. Ion Processes* **1986**, *72*, 187–194.
(23) Chen, L.; Cottrell, C. E.; Marshall, A. G. *Chemom. Intell. Lab. Syst.* **1986**, *1*, 51–58.
(24) Devore, J. L. *Probability and Statistics for Engineering and the Sciences*; Brooks/Cole: Monterey, CA, 1982; p 197.
(25) Press, W. H.; et al. *Numerical Recipes*; Cambridge University: New York, 1986; pp 191–203.

RECEIVED for review June 13, 1989. Accepted October 18, 1989. This work was supported by grants (to A.G.M.) from the U.S.A. Public Health Service (N.I.H. GM-31683) and The Ohio State University.